A&A 448, 165–169 (2006)
DOI: 10.1051/0004-6361:20054459

Astronomy & Astrophysics

[O III] profile substructure in radio–quiet quasars⋆

C. Leipski and N. Bennert

Astronomisches Institut Ruhr–Universität Bochum, Universitätsstrasse 150, 44780 Bochum, Germany
e-mail: [leipski;nbennert]@astro.rub.de

Received 27 July 2005 / Accepted 4 November 2005

ABSTRACT

Interactions between the radio jet and the optical emission of the narrow-line region (NLR) are a well known phenomenon in Seyfert galaxies. Here, we present the study of possible jet-NLR interactions in five radio-quiet PG quasars with double or triple radio structure. High spatial and spectral resolution observations were carried out in the Hβ-[O III] λ5007 wavelength range. In all cases, there is evidence for [O III] profile substructure (shoulders, subpeaks, blueshifted "broad" components) with different clarity. To measure the velocity, line width, intensity, and location of these [O III] components, several Gaussians were fitted. Often, the substructures are more pronounced close to the radio lobes, suggestive of jet-NLR interactions. Our observations support the unification scheme in which radio-quiet quasars are assumed to be the luminous cousins of Seyfert galaxies.

Key words. galaxies: active – galaxies: quasars: emission lines – galaxies: jets

1. Introduction

The narrow [O III] λ5007 emission typical for active galactic nuclei (AGNs) originates from the ionized narrow-line region (NLR) gas surrounding the luminous central engine, most likely an accreting supermassive black hole (BH).

For Seyfert galaxies, significant progress has been made in the past few years in understanding the physics of the NLR and revealed a close interaction between the radio jet and the NLR gas. Both the radio-emitting region and the NLR have comparable sizes and often show a closely matching morphology. The radio structure is known in many cases to comprise linear double or triple sources (Ulvestad & Wilson 1984a,b; Schmitt et al. 2001) and the emission-line morphologies often show a rich variety such as strands or bow-shock like structures (Falcke et al. 1998; Whittle et al. 2004).

Whittle et al. (1988) observed ten Seyfert galaxies with aligned multiple radio structures and found clear evidence for [O III] profile substructure, often coinciding with the position of radio lobes. The presence of two line emitting constituents in the NLR ("ambient [O III]" which displays an apparently normal rotational velocity field as well as kinematically displaced "[O III] components" which are intimately associated with individual radio lobes) are interpreted as clear signatures of the interaction of the radio jet with the dense surrounding interstellar medium, supporting the findings from imaging campaigns.

While quasars are assumed to be the luminous cousins of Seyfert galaxies, there is a significant lack of comparable dedicated quasar NLR studies. Most comparable studies of high-luminosity AGN focus on radio-loud objects, using pure radio or emission-line imaging to test radio-NLR alignments. There are only a few detailed spectroscopic studies of the jet gas-interactions of radio galaxies (e.g. Clark et al. 1997, 1998) or compact steep-spectrum sources (e.g. Gelderman & Whittle 1994; Chatzichristou et al. 1999), including quasars. All of these sources have radio luminosities (and therefore suspected jet energies) that are a few orders of magnitude greater than in Seyferts, possibly altering the interaction scenario significantly.

Bennert et al. (2002) performed the first comprehensive HST study of structure and morphology of a well-selected sample of seven radio-quiet Palomar Green (PG) quasars, observed in [O III]. All seven quasars revealed extended [O III] emission. Additionally, Leipski et al. (2006) present high sensitivity radio-maps of radio-quiet quasars (RQQ; including those of Bennert et al. 2002) and Seyfert galaxies to investigate the jet-NLR interaction by comparing their morphologies: There is a striking similarity of the radio and [O III] images suggesting equally pronounced jet-NLR interactions in both types of objects.

Here, we explore the interaction scenario of radio-jet and NLR gas in RQQ in a pilot study of five objects by means of long-slit spectroscopy.

2. Observation and reduction

High spatial resolution long-slit spectra of five radio-quiet PG quasars (PG 0157+001, PG 1012+008, PG 1119+120,

⋆ Based on observations made with ESO Telescopes at the La Silla Observatory under programme ID 73.B–0290.

Table 1. Observations.

Object	z^a	integration	PA	seeing	pc/″
PG 0157+001	0.162	3600 s	106°	<0.″7	2750
PG 1012+008	0.186	3600 s	142°	<1″	3110
PG 1119+120	0.049	3600 s	53°	<1″	985
PG 1149−110	0.048	3600 s	78°	<0.″7	965
PG 1307+085	0.154	4800 s	112°	<0.″7	2660

[a] From the peak velocity of the broad Hβ line.

PG 1149−110, and PG 1307+085) were obtained using EMMI attached to the Nasmyth B focus of the ESO-NTT. Observations were made in the Hβ/[O III] spectral range through the nucleus of each quasar with exposure times of ∼60 min in total and a typical seeing of <1″ (see Table 1 for details). The spatial resolution element is 0.″3 pix^{-1}, the nominal spectral resolution 0.4 Å pix^{-1}. The slit width used corresponds to 0.″5 on the sky projecting to a spectral resolution of ∼0.9 Å (∼50 km s^{-1} at 5300 Å) as measured by the full width at half maximum (*FWHM*) of comparison lines and night-sky lines. The long-slit used corresponds to 200″ in the sky and was orientated along the position angle (PA) of the maximum extent in the [O III] or radio image as determined from the images of Bennert et al. (2002) and Leipski et al. (2006).

Standard reduction including bias subtraction, flat-field correction, cosmic-ray removal, wavelength, and flux-calibration was performed using the ESO-MIDAS software (version Feb. 04).

To check the contribution of any Fe II emission at 4924 Å and 5018 Å, we followed the procedure of Peterson et al. (1981), using the λ4570 blend as an estimate of the Fe II emission. We find that the Fe II emission is neglible. Moreover, a significant contribution of Fe II emission at 4924 Å and 5018 Å would make the two [O III] lines asymmetric in the opposite senses, what is not observed here.

Two to three rows were averaged from the frames according to the seeing to enhance the S/N without loosing any spatial information. Thus, each "resulting row" corresponds to 0.″7 or 1.″0 along and 0.″5 perpendicular to the slit direction, respectively. Along the "spatial axis" of the CCD, we identified the "photometric center" (that we choose as "zero" on the spatial scale) with that spectral row of the CCD where the continuum is at maximum ("central row"). The linear scales (pc/″) were calculated using the velocity relative to the 3 K background, $H_0 = 71$ km s^{-1} Mpc^{-1} and a world model in agreement with the recent results of the Wilkinson Microwave Anisotropy Probe (Bennett et al. 2003).

Velocities, line widths, and intensities of the different [O III] components were measured as a function of distance from the nuclei by fitting Gaussians to the line profile.

In a first attempt, we tried to fit the [O III] λ5007 line with the least number of Gaussians. This set of Gaussians was extended to also fit [O III] λ4959 (with a fixed flux ratio of 3:1). The parameters of the successful fit were then used to fit Hβ, taking into account only those components of the [O III] fit with a significant contribution to the Hβ line (peak values as free parameters). Additionally, we included a broad component without constraints.

3. Results and discussion

In the following, we present the results on an object-by-object basis. The central spectra with the fitted components are shown in Fig. 1. We were not able to estimate the excitation (as measured from the [O III]/Hβ ratio) for all components due to dilution by the broad Hβ line. While the broad emission is especially strong in the nuclear spectrum, we were limited by a lack of signal in the outer spectra. Moreover, in all five quasars the [O III] line is (significantly) stronger than Hβ (Fig. 1) and we were often limited by a noisy (or even absent) Hβ line. For those [O III] components which could be identified and fitted in the Hβ line, we give the ratios in the text. The different components have on average high [O III]/Hβ values (∼5–8), consistent with photoionization by the AGN.

3.1. PG 0157+001

This radio-quiet quasar at a redshift of $z = 0.163$ (Table 1) comprises a triple radio source and shows exceptional structures in the HST [OIII] emission-line images (Bennert et al. 2002). Being well aligned with the radio structure, the [OIII] emission displays a prominent bow-shock like arc on the western side of the nucleus suggesting strong jet-NLR interaction. On the eastern side, an emission blob is lying at the same distance from the nucleus as the radio knot (∼0.″7) but slightly displaced to the north (∼0.″5) (Leipski et al. 2006). On larger scales (∼6″), Stockton & MacKenty (1987) show extended emission-line features in their ground-based observations that closely resembles the structures seen on small scales.

We aligned the long-slit with these larger structures and indeed detect extended emission on similar scales. However, the low S/N does not allow a detailed line fitting. Nevertheless, some basic parameters can be determined: The excitation of the north-western emission is twice as high as that of the south-eastern region ([O III]/Hβ = 7.2 vs. 3.3). There is a small velocity shift between the south-eastern and the north-western extended emission (∼80 km s^{-1}). It is not clear whether this velocity difference can be interpreted as galactic rotation or is due to outflowing gas with the western region pointing towards us.

In the central part (inner ∼3″), we study radially varying properties. The [O III] line can be best fitted by a two-component system (Fig. 1). As the blue-shifted component is not seen in the Hβ line, it indicates a high excitation ([O III]/H$\beta \geq 11$) of this very broad (∼1400 km s^{-1}) feature. As can be seen in Fig. 2, this broad [O III] component is most prominent in the center, slowly fades out to the south-east, and evolves into a pronounced and much narrower (∼560 km s^{-1}) secondary peak ∼1.″4 from the center in the north-west at a blueshifted velocity of ∼1200 km s^{-1}. This position corresponds to the bow-shock like structure in the emission-line gas

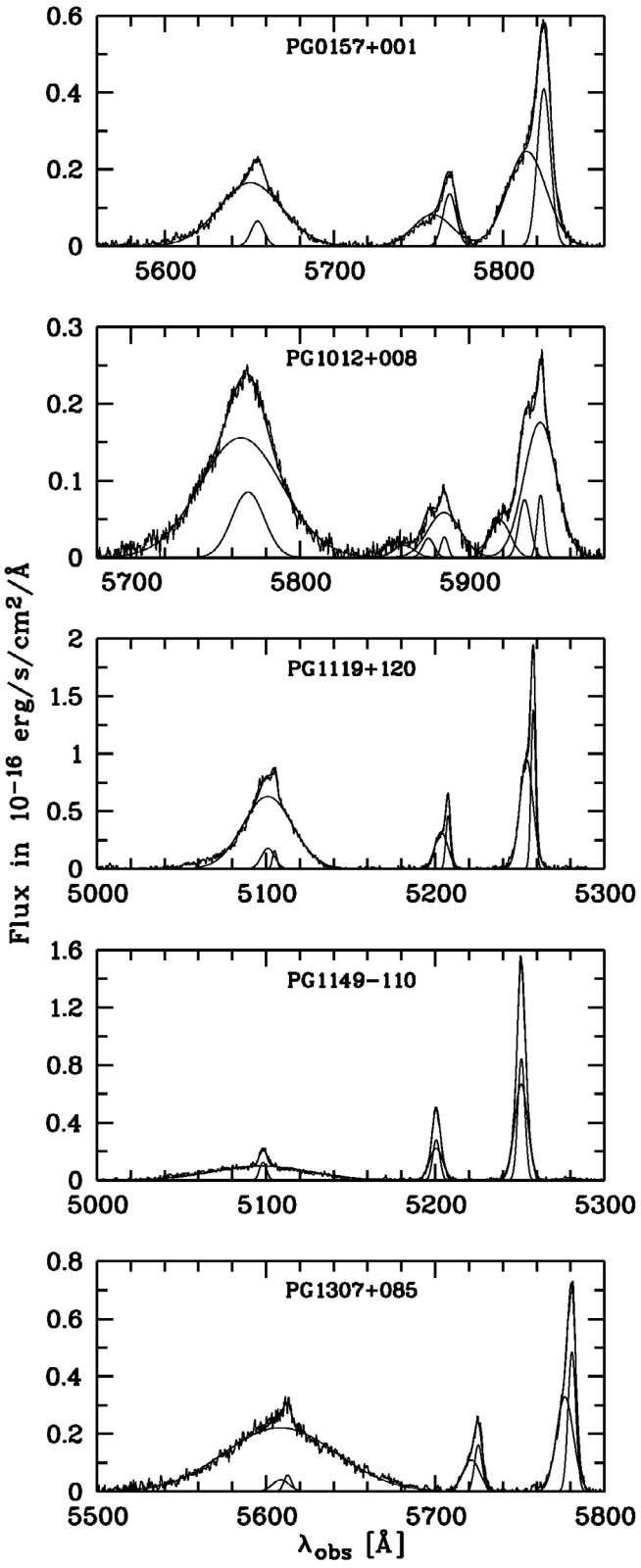

Fig. 1. Central spectra of the five PG quasars. The observed spectrum is shown, overlayed with the fitted components as well as with the total fit.

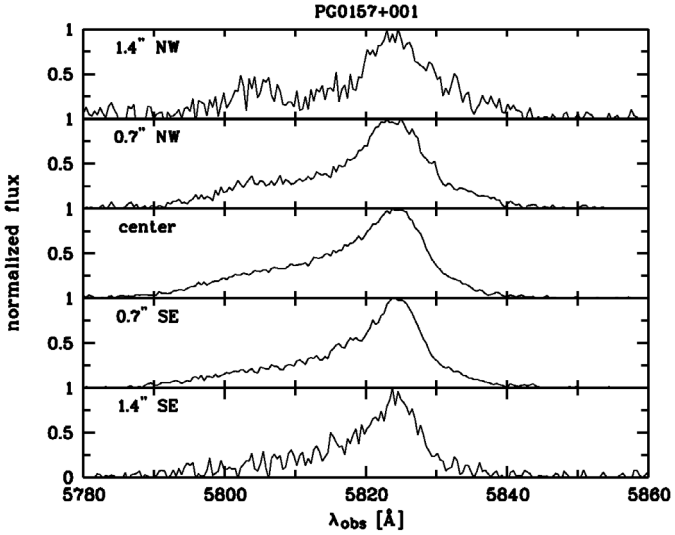

Fig. 2. Spatial sequence of spectra of PG 0157+001.

distribution (Bennert et al. 2002), also coinciding with the radio knot observed by Leipski et al. (2006). These findings strongly suggest an interaction of the radio ejecta with the emission-line gas, which is swept-up and driven outwards (towards the observer) by the jet, thus creating the bow-shock.

Note that additional components may possibly be seen in the [O III] emission-line profile of PG 0157+001 (e.g. a red wing or a component in between the two fitted ones visible at 1.″4 north-west, Fig. 2). These components were included in the fit on an individual row-by-row basis, but no consistent fitting scenario could be found for all rows. This indicates that the radial variations of the line profile are more complex.

3.2. PG 1012+008

The quasar PG 1012+008 is merging with a nearby companion (Bahcall et al. 1997). This complicates the interpretation of the profile substructures which may be either caused by the merger or by the radio jet. The radio structure of PG 1012+008 consists of a central source with a ∼1.″5 long bent jet to the south-east. The emission-line gas is distributed rather uniformly, but the shape of the isophotes resembles that of the radio structure (Leipski et al. 2006).

In our spectra, the object exhibits a wealth of structure in the [O III] profile (Fig. 1). A blue component is displaced by nearly 1000 km s^{-1} with respect to the peak suggesting a fast outflow. While this component is detected in the inner 3″, it is most prominent in the center compared to the peak of the total profile. The observed emission is confined to these 3″ and the profiles do not vary significantly with distance from the center. However, the blue asymmetry seen in the central [O III] profile becomes a red asymmetry towards the south of the nucleus, indicative of material flowing in south-eastern direction. This coincides with the direction of the radio jet. Moreover, the [O III] emission-line image of this source shows elongated isophotes in the very same direction. Whether the observed outflow can be attributed to a radio jet originating in the active nucleus or is influenced by the merger event cannot be answered at present. We suggest that the outflow itself is powered by the active nucleus but the extended distribution of the gas seen in

the [O III] image as well as the "bent" shape of the jet is due to the interaction of the two galaxies.

3.3. PG 1119+120

PG 1119+120 shows radio structures of ∼5″ diameter. On the eastern side of the nucleus, a jet sharply bends to the north at a distance of 2.″5, while a single radio knot is detected on the western side (Leipski et al. 2006). We extract spectra on similar scales. The central spectrum of this source reveals a two-component [O III] line with both components visible in the Hβ line as well. The radial variations are most obvious towards the south-west: While the narrower, red component has a stable [O III]/Hβ ratio (∼8), the excitation of the blue-shifted broader component increases by 40% from the nucleus out to ∼1.″5 (SW) ([O III]/Hβ ∼ 5.3 to 8.7). Similarly, while the flux in both components equals at that distance (which coincides with the position of the western radio knot), the red component is stronger in the nucleus by a factor of 2. The presence of the radio knot and the increasing flux of the blue-shifted component indicate strong jet-NLR interaction in the south-west of the nucleus.

According to its velocities, the narrower, red component seems to represent ambient [O III] emission that follows galactic rotation, while the (variable) blueshifted [O III] component is most likely attributed to gas motions caused by the radio ejecta. Interestingly, no remarkable [O III] substructures are visible at the location of the north-eastern radio jet that is much more pronounced in the radio regime.

3.4. PG 1149−110

Although this object shows extended structures in the radio regime, no significant [O III] profile substructure can be seen (Fig. 1). Nevertheless, two Gaussians are needed to fit the observed profile due to broader wings, a phenomenon already known from Seyfert galaxies (e.g. Whittle et al. 1985; Verón-Cetty et al. 2001; Schulz & Henkel 2003; Bennert et al. 2004). We were not able to extract more than 3 spectra (diameter ∼ 2″) at a $S/N > 3$. PG 1149−110 shows that the presence of extended radio emission alone does not necessarily imply significant profile substructure in the [O III] lines. This may indicate that the extended radio emission suggestive of radio jets expands nearly perpendicular with respect to the observer resulting in an absence of pronounced [O III] components. However, there are signs of a red asymmetry at ∼1″ east, at the location of the eastern radio knot (Leipski et al. 2006) indicating interaction.

3.5. PG 1307+085

The host galaxy of PG 1307+085 is classified as a small early-type galaxy (Bahcall et al. 1997) and, like PG 0157+001, this is a quasar in our sample that shows remarkable spatially varying [O III] profile substructure: In the center and towards the north-west, the [O III] profile consists of a narrow central component with a broad blue shoulder (Fig. 1). From 0.″7 to 2.″8 south-east,

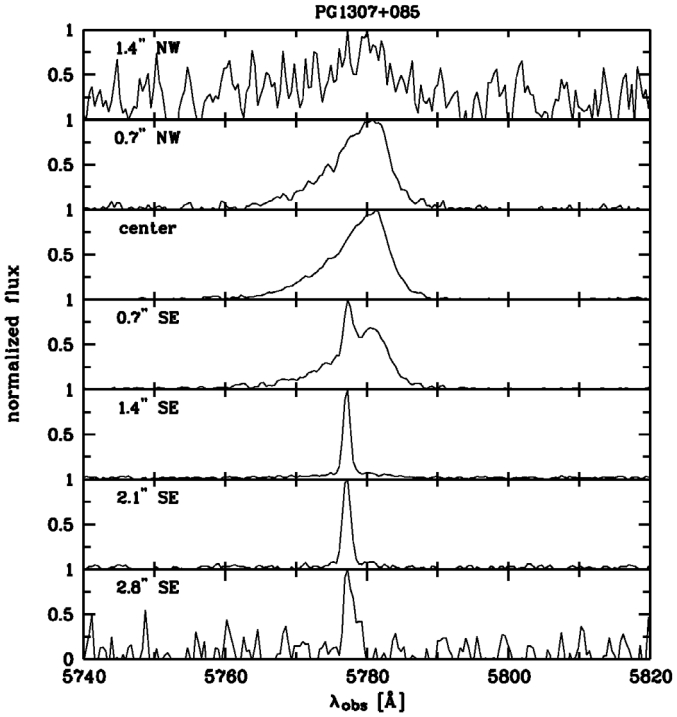

Fig. 3. Spatial sequence of spectra of PG 1307+085.

an additional narrow component appears which is not visible in the other rows (Fig. 3). The presence of this component in the central rows is difficult to assess because of the presence of the broad component which is much stronger. However, on the other side of the nucleus at 0.″7 north-west, it may reflect in a weak shoulder bluewards of the peak of the line profile. We identify this component with ambient [O III] gas in the host galaxy. The emission-line of the ambient gas is very narrow (∼1 Å ∼69 km s^{-1}) and shows no significant velocity shift.

4. Conclusions

In all five observed radio-quiet PG quasars, we find evidence for [O III] profile substructure with different clarity. Often, this substructure is pronounced at the location of the radio lobes. This suggests that at least part of the emission-line gas is intimately associated with individual radio lobes, indicating a close NLR-jet interaction. However, the presence of radio lobes does not necessarily lead to the presence of pronounced [O III] profile substructure. The orientation of the radio-jet with respect to the observer seems to be a crucial factor for enhanced profile substructure. Our results are comparable with similar studies of Seyfert galaxies (e.g. Whittle et al. 1988) and support the unification scheme in which radio-quiet quasars are assumed to be the luminous cousins of Seyferts. However, the excitation as measured from the [O III]/Hβ ratio turns out to be generally lower for our quasars (∼5–8) than for Seyfert galaxies (∼10–12, Whittle et al. 1988).

Acknowledgements. C.L. was supported by Sonderforschungsbereich SFB 591 "Universelles Verhalten gleichgewichtsferner Plasmen" der Deutschen Forschungsgemeinschaft. N.B. is grateful for financial support by the "Studienstiftung des deutschen Volkes". We also acknowledge the helpful comments of the anonymous referee. We

thank Mark Whittle for useful suggestions helping to improve the paper.

References

Bahcall, J. N., Kirhakos, S., Saxe, D. H., & Schneider D. P. 1997, ApJ, 479, 642
Bennert, N., Falcke, H., Schulz, H., Wilson, A. S., & Wills, B. J. 2002, ApJ, 574, L105
Bennert, N., Schulz, H., & Henkel, C. 2004, A&A, 419, 127
Bennett, C. L., Halpern, M., Hinshaw, G., et al. 2003, ApJS, 148, 1
Chatzichristou, E. T., Vanderriest, C., & Jaffe, W. 1999, A&A, 343, 407
Clark, N. E., Tadhunter, C. N., Marganto, R., et al. 1997, MNRAS, 286, 558
Clark, N. E., Axon, D. J., Tadhunter, C. N., Robinson, A., & O'Brien, P. 1998, ApJ, 494, 546
Falcke, H., Wilson, A. S., & Simpson, C. 1998, ApJ, 502, 199
Gelderman, R., & Whittle, M. 1994, ApJS, 91, 491
Leipski, C., Falcke, H., Bennert, N., & Hüttemeister, S. 2006, A&A, submitted
Peterson, B. M., Foltz, C. B., & Byard, P. L. 1981, ApJ, 243, L61
Schmitt, H., Ulvestad, J. S., Antonucci, R. R. J., & Kinney, A. L. 2001, ApJS, 132, 199
Schulz, H., & Henkel, C. 2003, A&A, 400, 41
Stockton, A., & MacKenty, J. W. 1987, ApJ, 316, 584
Ulvestad, J. S., & Wilson, A. S. 1984a, ApJ, 278, 544
Ulvestad, J. S., & Wilson, A. S. 1984b, ApJ, 285, 439
Verón-Cetty, M.-P., Verón, P., & Gonçalves, A. C. 2001, A&A, 372, 730
Whittle, M. 1985, MNRAS, 213, 1
Whittle, M., & Wilson, A. S. 2004, AJ, 127, 606
Whittle, M., Pedlar, A., Meurs, E. J. A., et al. 1988, ApJ, 326, 125